Supporting Information for

Novel alkaline earth metal-organic frameworks with thiophene group for selective Detection of Fe^{3+}

Jun Yao, Yan-E Liu, Li-Bo Yang, Ai-Na Dou, Cheng-Fu Hou, Quan-Qing Xu, Bo Huang* and Ai-Xin Zhu*

Faculty of Chemistry and Chemical Engineering, Yunnan Normal University, Kunming 650500, China.

E-mail: huangbo15@foxmail.com (Bo Huang) and zaxchem@126.com (Ai-Xin Zhu);.

.

Table S1 Crystal data and structure refinements for **1-3**

Compounds	**1**	**2**	**3**
Formula	$C_{29}H_{37}Mg_2N_3O_{13}S_4$	$C_{13}H_{13}CaNO_5S_2$	$C_{13}H_{13}NO_5S_2Sr$
Formula weight	812.47	367.44	414.98
Crystal system	Monoclinic	Orthorhombic	Orthorhombic
Space group	$P2_1/m$	$Pmc2_1$	$Pnma$
a (Å)	10.759(2)	22.642(3)	7.3261(15)
b (Å)	19.330(4)	9.7853(12)	22.720(5)
c (Å)	12.307(3)	6.8909(8)	9.936(2)
α (deg)	90	90	90
β (deg)	100.26(3)	90	90
γ (deg)	90	90	90
V (Å^3)	2518.7(9)	1526.7(3)	1653.8(6)
Z	2	4	4
D_c (g·cm^{-3})	1.071	1.599	1.667
μ (mm^{-1})	0.262	0.706	3.532
GOF	1.064	1.115	1.243
R_1 [$I > 2\sigma(I)$]^a	0.1072	0.0393	0.0660
WR_2 [$I > 2\sigma(I)$]^b	0.3159	0.1070	0.1625
R_1 [all data]	0.1944	0.0412	0.0742
wR_2 [all data]	0.3707	0.1092	0.1679
Diff peak, hole (e Å^{-3})	0.761, -0.394	0.458, -0.344	0.958, -0.852

$R_1 = \sum||F_o| - |F_c||/\sum|F_o|$. $wR_2 = [\sum w(F_o^2 - F_c^2)^2/\sum w(F_o^2)^2]^{1/2}$

Table S2 Selected bond lengths(Å) and angles(°) for **1**.

Mg(1)-O(1)	2.069(4)	Mg(1)-O(1W)	2.161(6)
Mg(1)-O(1)#1	2.069(4)	Mg(1)-O(2W)	2.052(8)
Mg(1)-O(3)	2.075(4)	Mg(1)-O(3)#1	2.075(4)
Mg(2)-O(1W)	2.074(5)	Mg(2)-O(2)	2.025(5)
Mg(2)-O(2)#1	2.025(5)	Mg(2)-O(5)	2.053(6)
Mg(2)-O(6)	2.034(6)	Mg(2)-O(6)#1	2.034(6)
O(1)-Mg(1)-O(1)#1	92.6(2)	O(1)-Mg(1)-O(1W)	91.30(19)
O(1)-Mg(1)-O(3)	88.34(16)	O(1)-Mg(1)-O(3)#1	178.97(19)
O(1)#1-Mg(1)-O(1W)	91.30(19)	O(1)#1-Mg(1)-O(3)	178.97(19)
O(1)#1-Mg(1)-O(3)#1	88.34(16)	O(2W)-Mg(1)-O(1)	88.1(2)
O(2W)-Mg(1)-O(1)#1	88.1(2)	O(2W)-Mg(1)-O(1W)	179.2(2)
O(2W)-Mg(1)-O(3)	91.4(2)	O(2W)-Mg(1)-O(3)#1	91.4(2)
O(3)-Mg(1)-O(1W)	89.15(19)	O(3)-Mg(1)-O(3)#1	90.7(2)
O(3)#1-Mg(1)-O(1W)	89.15(19)	O(2)-Mg(2)-O(1W)	92.8(2)
O(2)-Mg(2)-O(5)	90.7(2)	O(2)-Mg(2)-O(6)	88.7(2)
O(2)-Mg(2)-O(6)#1	177.4(3)	O(2)#1-Mg(2)-O(1W)	92.8(2)
O(2)#1-Mg(2)-O(2)	93.8(3)	O(2)#1-Mg(2)-O(5)	90.7(2)
O(2)#1-Mg(2)-O(6)	177.4(3)	O(2)#1-Mg(2)-O(6)#1	88.7(2)
O(5)-Mg(2)-O(1W)	174.9(3)	O(6)-Mg(2)-O(1W)	88.1(2)
O(6)-Mg(2)-O(5)	88.2(2)	O(6)-Mg(2)-O(6)#1	88.9(4)
O(6)#1-Mg(2)-O(1W)	88.1(2)	O(6)#1-Mg(2)-O(5)	88.2(2)

Symmetry code: #1: x, -y+1/2, z.

Table S3 Selected bond lengths(Å) and angles(°) for **2**.

Ca(1)-O(1)	2.402(4)	Ca(1)-O(1)#3	2.402(4)
Ca(1)-O(2)	2.604(4)	Ca(1)-O(2)#1	2.341(4)
Ca(1)-O(2)#2	2.341(4)	Ca(1)-O(2)#3	2.604(4)
Ca(1)-O(5)	2.468(5)	Ca(1)-O(5)#4	2.495(5)
Ca(2)-O(3)	2.633(4)	Ca(2)-O(3)#5	2.361(4)
Ca(2)-O(3)#6	2.361(4)	Ca(2)-O(3)#8	2.633(4)
Ca(2)-O(4)	2.410(4)	Ca(2)-O(4)#8	2.410(4)
Ca(2)-O(6)	2.437(5)	Ca(2)-O(6)#7	2.405(5)
O(1)-Ca(1)-O(2)	52.14(13)	O(1)-Ca(1)-O(2)#3	103.52(14)
O(1)-Ca(1)-O(5)	80.69(13)	O(1)-Ca(1)-O(5)#4	119.00(13)
O(1)#3-Ca(1)-O(1)	91.6(2)	O(1)#3-Ca(1)-O(2)	103.52(14)
O(1)#3-Ca(1)-O(2)#3	52.14(13)	O(1)#3-Ca(1)-O(5)	80.69(13)
O(1)#3-Ca(1)-O(5)#4	119.00(13)	O(2)-Ca(1)-O(2)#3	72.50(17)
O(2)#1-Ca(1)-O(1)	154.43(15)	O(2)#1-Ca(1)-O(1)#3	87.66(14)
O(2)#1-Ca(1)-O(2)	152.20(11)	O(2)#1-Ca(1)-O(2)#2	82.27(19)
O(2)#1-Ca(1)-O(2)#3	96.12(13)	O(2)#1-Ca(1)-O(5)	73.96(13)
O(2)#1-Ca(1)-O(5)#4	83.15(13)	O(2)#2-Ca(1)-O(1)	87.66(14)
O(2)#2-Ca(1)-O(1)#3	154.43(15)	O(2)#2-Ca(1)-O(2)	96.12(13)
O(2)#2-Ca(1)-O(2)#3	152.20(11)	O(2)#2-Ca(1)-O(5)	73.96(13)
O(2)#2-Ca(1)-O(5)#4	83.15(13)	O(5)-Ca(1)-O(2)	132.46(11)
O(5)-Ca(1)-O(2)#3	132.46(11)	O(5)-Ca(1)-O(5)#4	149.37(18)
O(5)#4-Ca(1)-O(2)	69.13(12)	O(5)#4-Ca(1)-O(2)#3	69.13(12)
O(3)-Ca(2)-O(3)#8	69.54(16)	O(3)#5-Ca(2)-O(3)	152.74(11)
O(3)#5-Ca(2)-O(3)#6	79.02(19)	O(3)#5-Ca(2)-O(3)#8	99.40(13)
O(3)#5-Ca(2)-O(4)	154.37(15)	O(3)#5-Ca(2)-O(4)#8	89.93(14)
O(3)#5-Ca(2)-O(6)	75.98(12)	O(3)#5-Ca(2)-O(6)#7	81.30(14)
O(3)#6-Ca(2)-O(3)	99.40(13)	O(3)#6-Ca(2)-O(3)#8	152.74(11)
O(3)#6-Ca(2)-O(4)	89.93(14)	O(3)#6-Ca(2)-O(4)#8	154.37(15)
O(3)#6-Ca(2)-O(6)	75.98(12	O(3)#6-Ca(2)-O(6)#7	81.30(14)
O(4)-Ca(2)-O(3)	51.56(12)	O(4)-Ca(2)-O(3)#8	100.82(14)
O(4)-Ca(2)-O(4)#8	90.4(2)	O(4)-Ca(2)-O(6)	78.95(12)
O(4)#8-Ca(2)-O(3)	100.82(14)	O(4)#8-Ca(2)-O(3)#8	51.56(12)
O(4)#8-Ca(2)-O(6)	78.95(12)	O(6)-Ca(2)-O(3)	130.46(11)
O(6)-Ca(2)-O(3)#8	130.46(11)	O(6)#7-Ca(2)-O(3)	71.61(13)
O(6)#7-Ca(2)-O(3)#8	71.61(13)	O(6)#7-Ca(2)-O(4)	120.11(13)
O(6)#7-Ca(2)-O(4)#8	120.11(12)	O(6)#7-Ca(2)-O(6)	150.39(17)

Symmetry codes: #1: -x+1, -y+2, z-1/2; #2: x, -y+2, z-1/2; #3: -x+1, y, z; #4: -x+1, -y+2, z+1/2; #5: -x+2, -y+1, z+1/2; #6: x, -y+1, z+1/2; #7: -x+2, -y+1, z-1/2; #8: -x+2, y, z.

Table S4 Selected bond lengths(Å) and angles(°) for **3**.

Sr(1)-O(1)	2.506(5)	Sr(1)-O(1)#1	2.506(5)
Sr(1)-O(1)#2	2.706(6)	Sr(1)-O(1)#3	2.706(6)
Sr(1)-O(2)#2	2.561(6)	Sr(1)-O(2)#3	2.561(6)
Sr(1)-O(3)	2.627(8)	Sr(1)-O(3)#4	2.566(8)
O(1)-Sr(1)-O(1)#1	78.0(3)	O(1)-Sr(1)-O(1)#2	153.56(13)
O(1)-Sr(1)-O(1)#3	99.3(2)	O(1)-Sr(1)-O(2)#2	154.9(2)
O(1)-Sr(1)-O(2)#3	90.2(2)	O(1)-Sr(1)-O(3)	83.8(2)
O(1)-Sr(1)-O(3)#4	73.94(19)	O(1)#1-Sr(1)-O(1)#2	99.3(2)
O(1)#1-Sr(1)-O(1)#3	153.56(13)	O(1)#1-Sr(1)-O(2)#2	90.2(2)
O(1)#1-Sr(1)-O(2)#3	154.9(2)	O(1)#1-Sr(1)-O(3)	83.8(2)
O(1)#1-Sr(1)-O(3)#4	73.94(19)	O(1)#2-Sr(1)-O(1)#3	71.3(3)
O(2)#2-Sr(1)-O(1)#2	49.67(18)	O(2)#2-Sr(1)-O(1)#3	100.8(2)
O(2)#2-Sr(1)-O(2)#3	91.5(4)	O(2)#2-Sr(1)-O(3)	117.19(18)
O(2)#2-Sr(1)-O(3)#4	81.60(19)	O(2)#3-Sr(1)-O(1)#2	100.8(2)
O(2)#3-Sr(1)-O(1)#3	49.67(18)	O(2)#3-Sr(1)-O(3)	117.19(18)
O(2)#3-Sr(1)-O(3)#4	81.60(19)	O(3)-Sr(1)-O(1)#2	69.77(18)
O(3)-Sr(1)-O(1)#3	69.77(18)	O(3)#4-Sr(1)-O(1)#2	131.12(16)
O(3)#4-Sr(1)-O(1)#3	131.12(16)	O(3)#4-Sr(1)-O(3)	151.2(2)

Symmetry codes: #1: x, -y+3/2, z; #2: x+1/2, -y+3/2, -z+1/2; #3: x+1/2, y, -z+1/2; #4: x-1/2, y, -z+1/2;

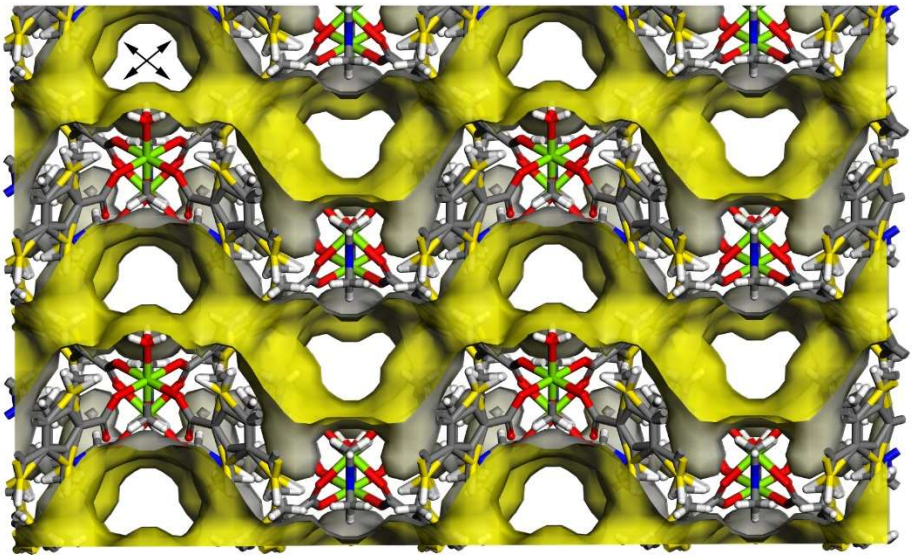

Fig. S1 View of the 3D framework and channel structure of **1** along the *c*-axis; 1D channel with an effective pore size of approximately 4.9 × 4.9 Å^2.

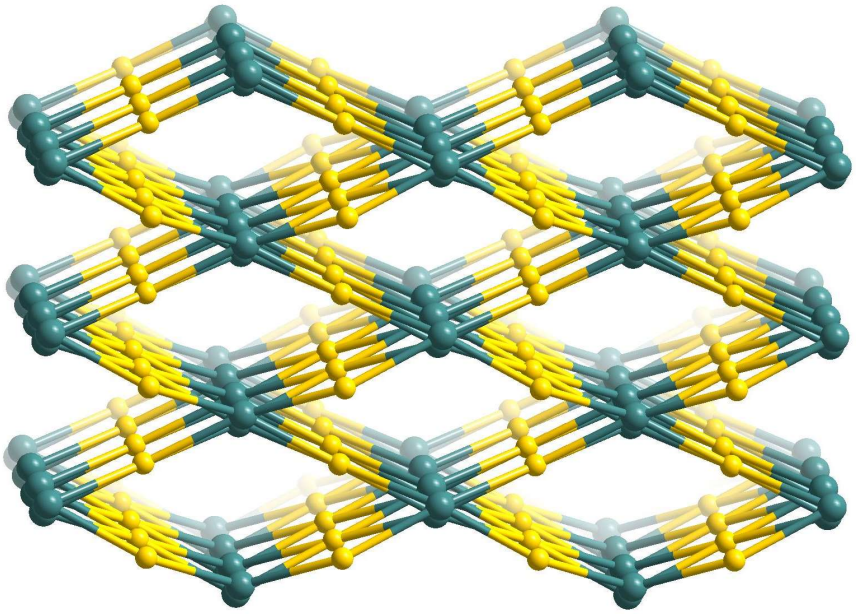

Fig. S2 Topological representation of the 4-connected lvt net of **3**.

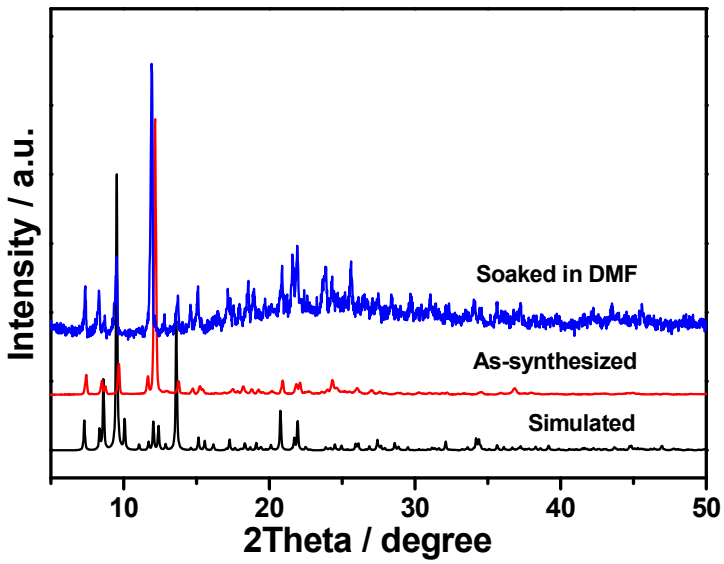

Fig. S3 PXRD patterns of **1** and **1** after soaking in DMF for 2 days.

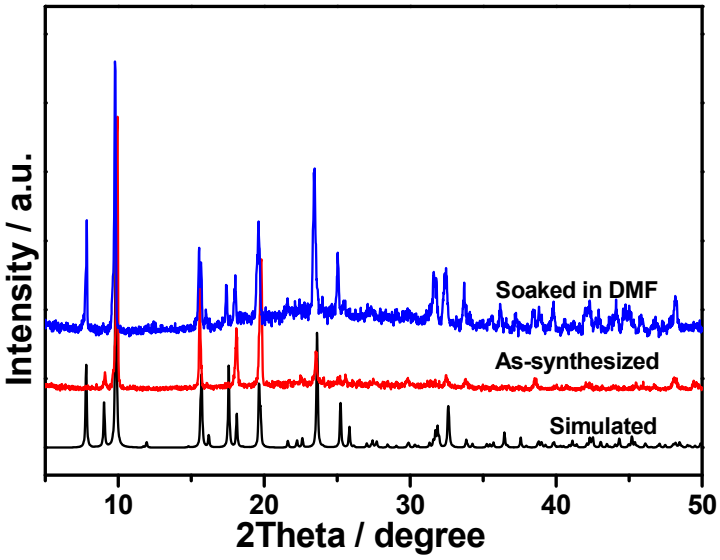

Fig. S4 PXRD patterns of **2** and **2** after soaking in DMF for 2 days. The differences of peak intensity between the simulated and as-synthesized patterns may be due to the preferred orientation of the powder samples.[1]

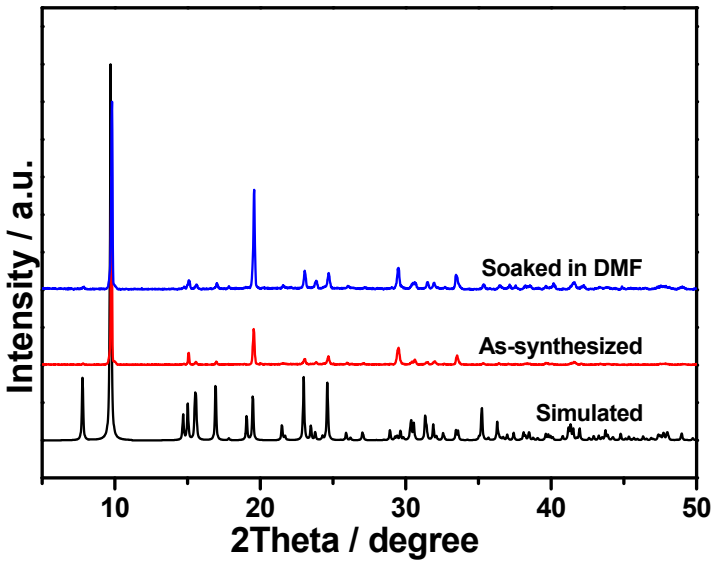

Fig. S5 PXRD patterns of **3** and **3** after soaking in DMF for 2 days.

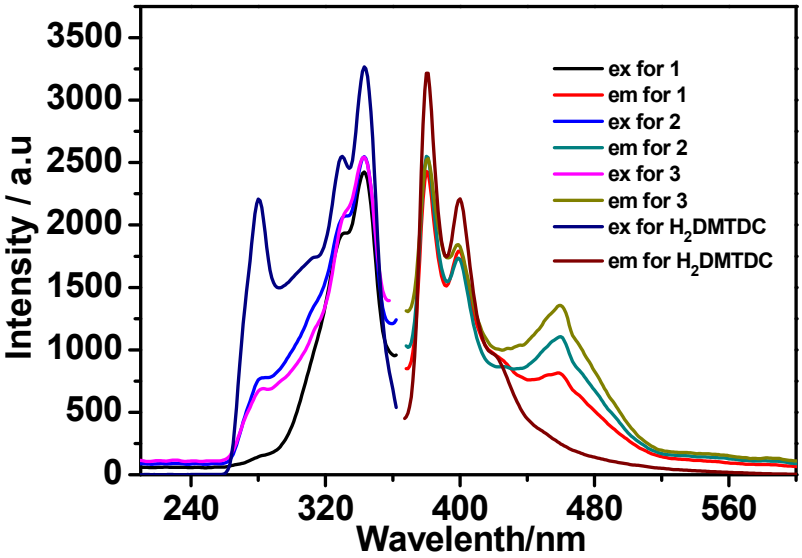

Fig. S6 The excitation and emission spectra of the ligand H_2DMTDC, **1**, **2** and **3** (dispersed) in DMF.

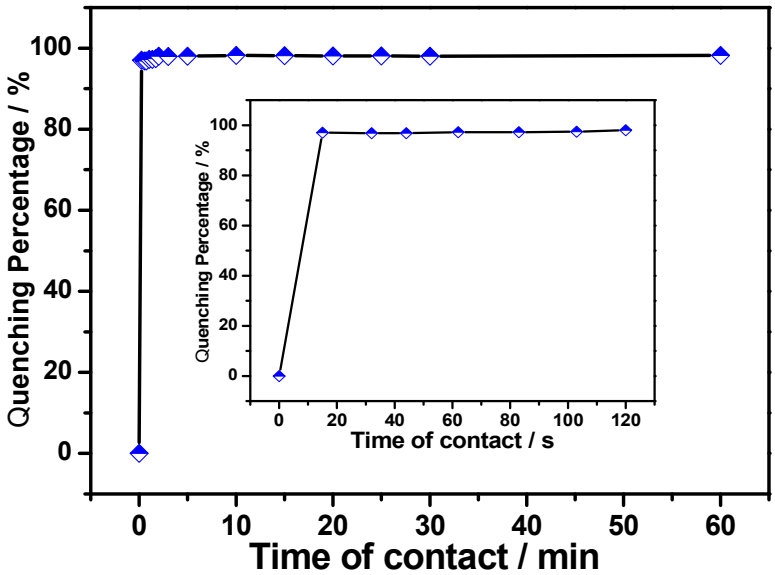

Fig. S7 Time-dependent fluorescence quenching by Fe^{3+} of **2**

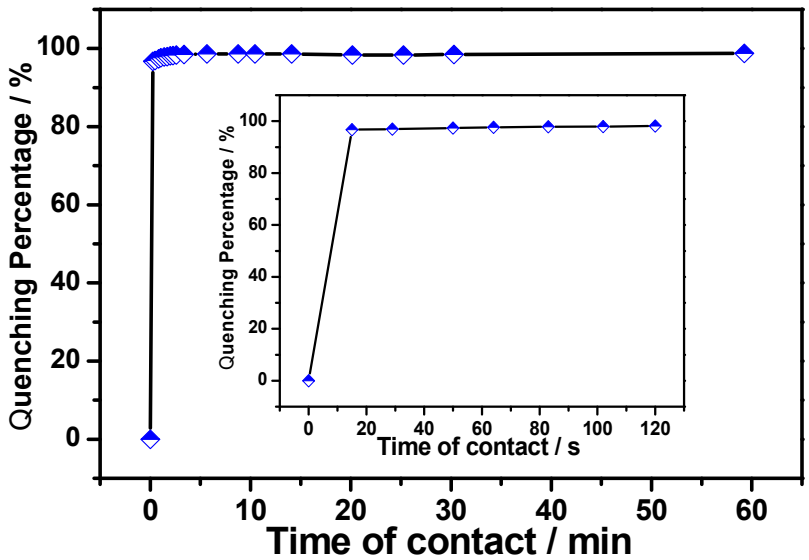

Fig. S8 Time-dependent fluorescence quenching by Fe^{3+} of **3**

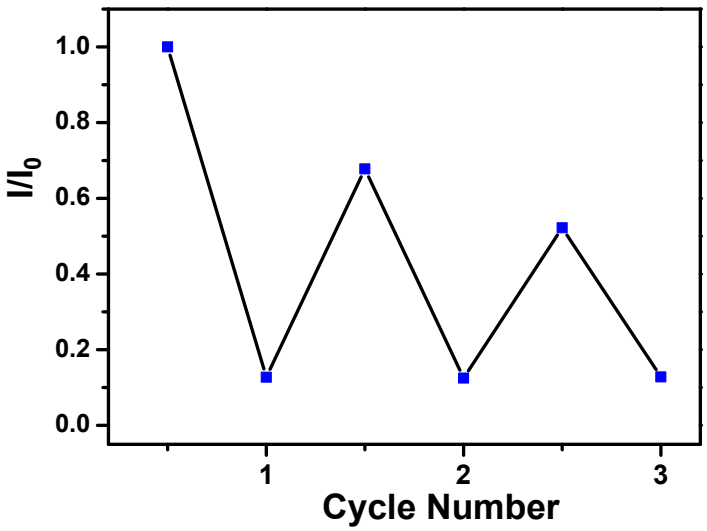

Fig. S9 Recyclability tests of **1** in the presence of Fe^{3+} washed only with DMF

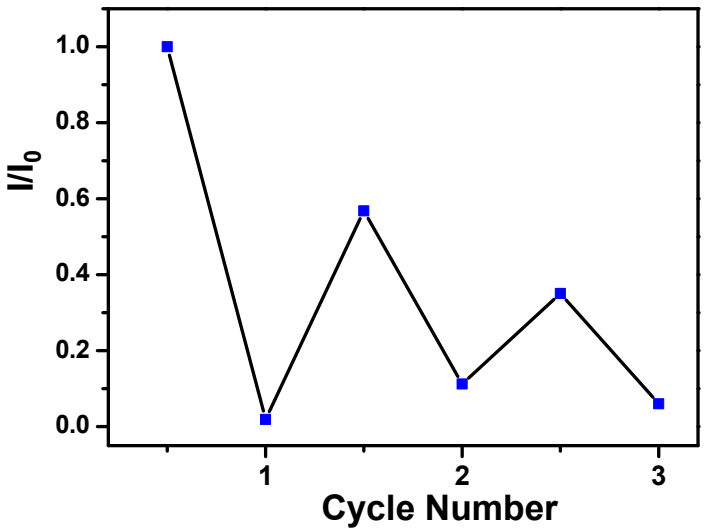

Fig. S10 Recyclability tests of **2** in the presence of Fe^{3+} washed only with DMF

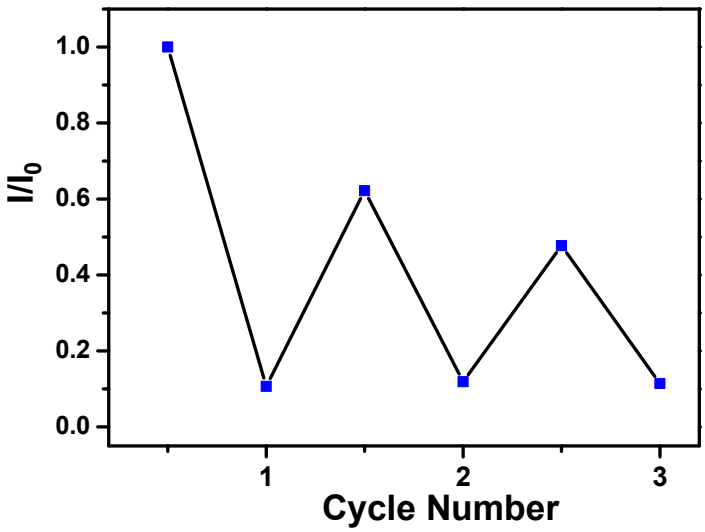

Fig. S11 Recyclability tests of **3** in the presence of Fe^{3+} washed only with DMF

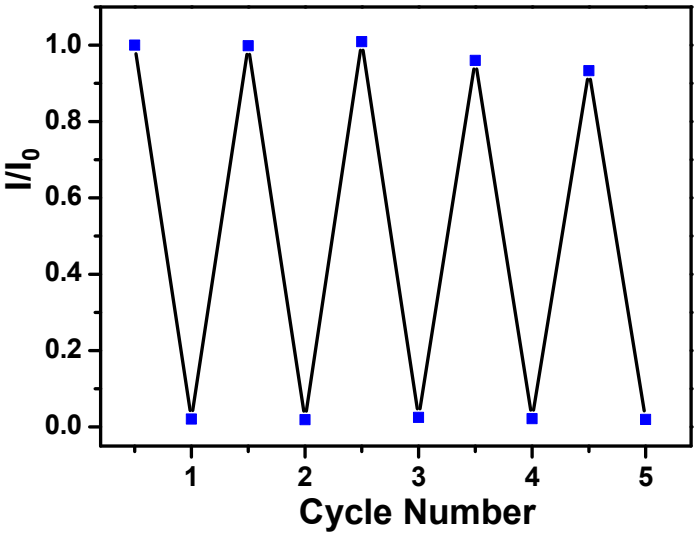

Fig. S12 Recyclability tests of **2** in the presence of Fe^{3+}

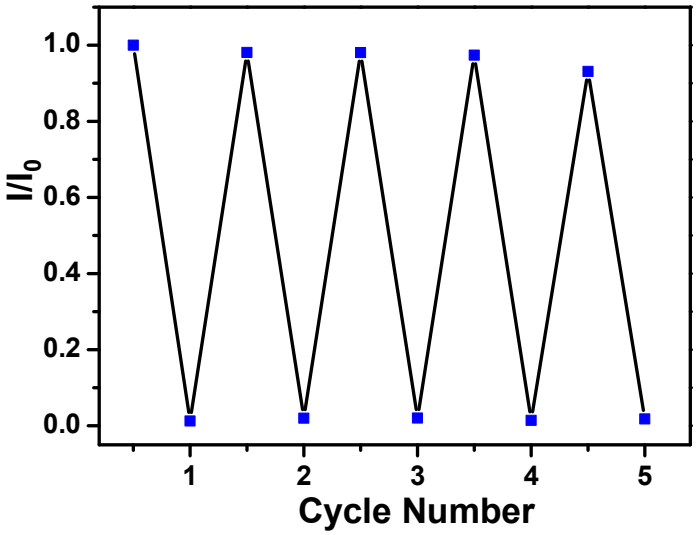

Fig. S13 Recyclability tests of **3** in the presence of Fe^{3+}

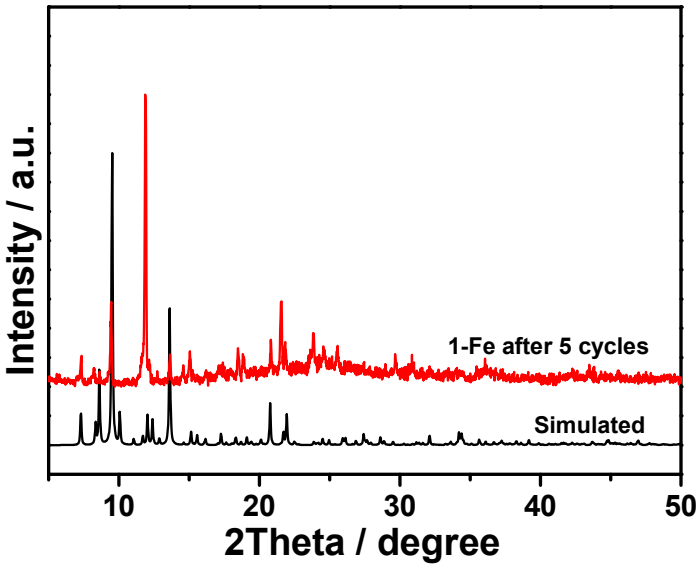

Fig. S14 XRD patterns of **1** after 5 cycles for sensing Fe^{3+}

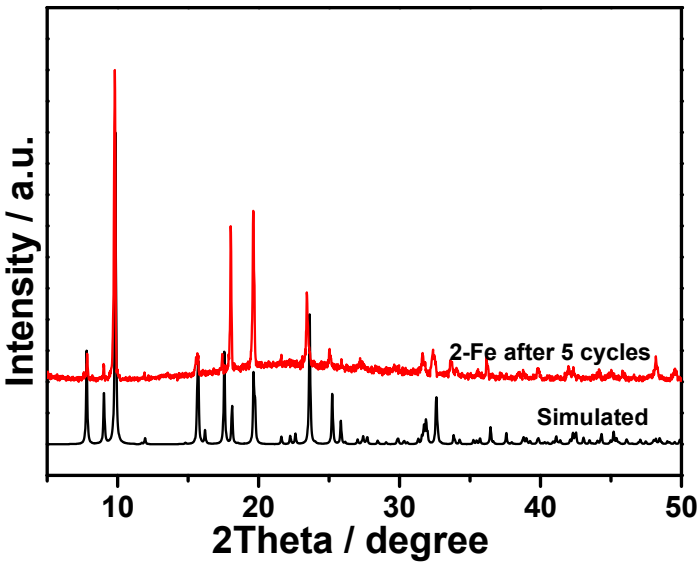

Fig. S15 XRD patterns of **2** after 5 cycles for sensing Fe^{3+}

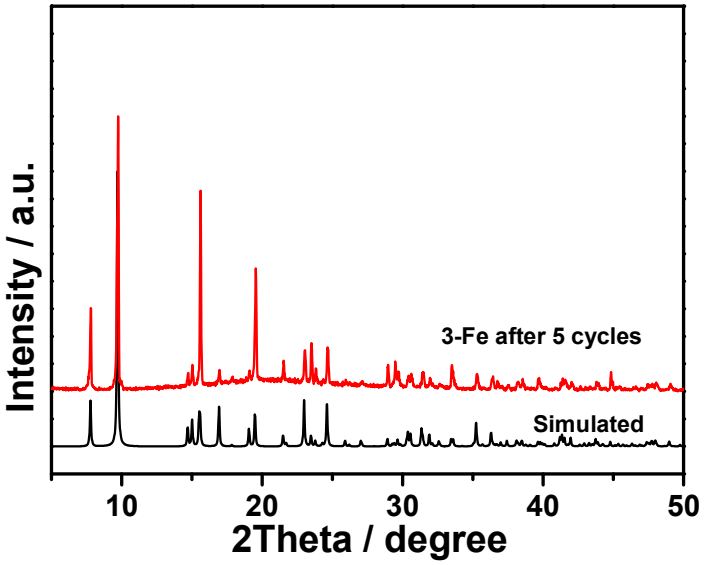

Fig. S16 XRD patterns of **3** after 5 cycles for sensing Fe^{3+}

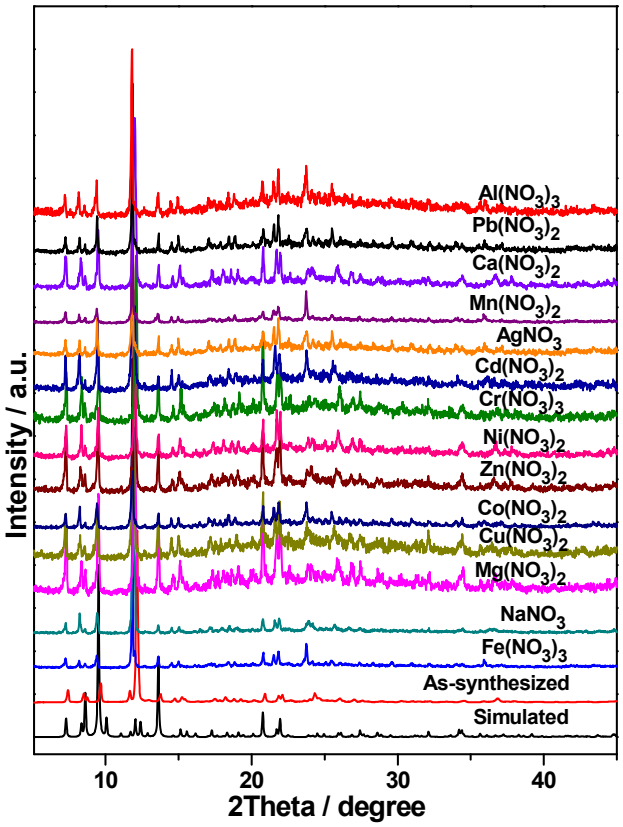

Fig. S17 PXRD of **1** after soaking different metal ions for 24 hrs in DMF

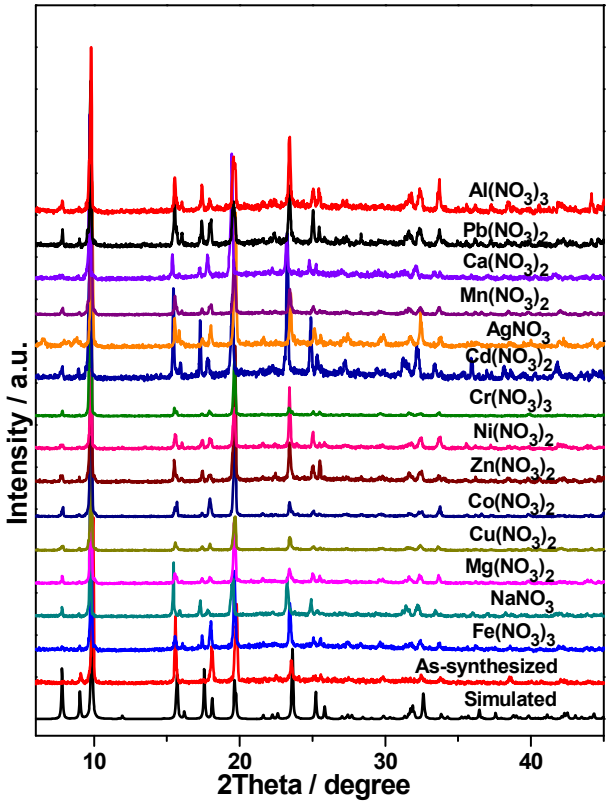

Fig. S18 PXRD of **2** after soaking different metal ions for 24 hrs in DMF

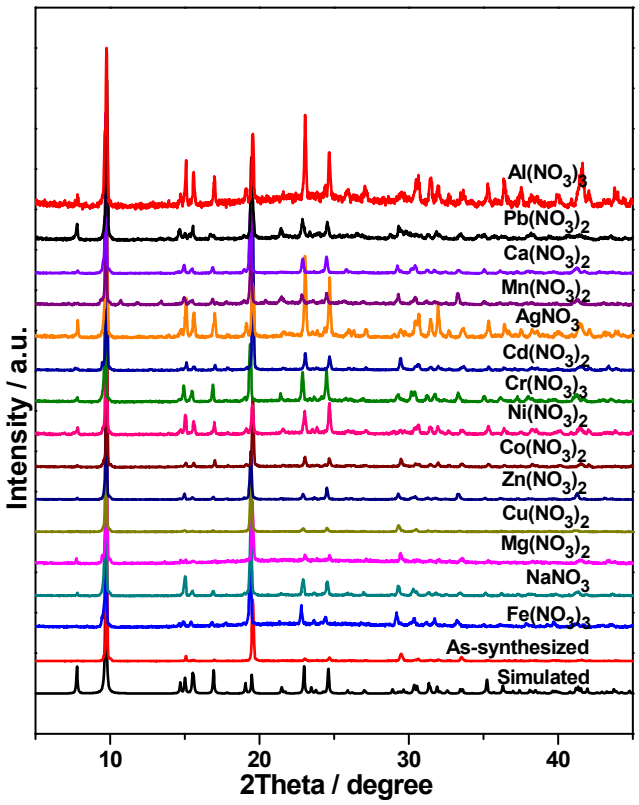

Fig. S19 PXRD of **3** after soaking different metal ions for 24 hrs in DMF

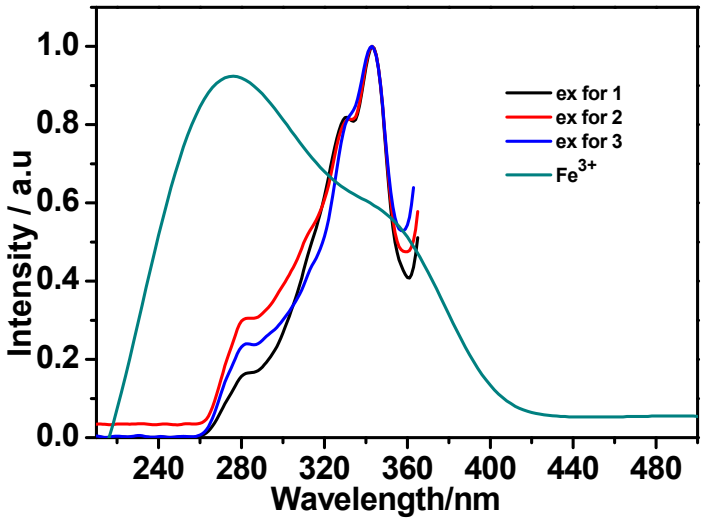

Fig. S20 The excitation spectra of **1**, **2** and **3** (dispersed in DMF) and UV-vis absorption spectrum of and $Fe(NO_3)_3$ in DMF

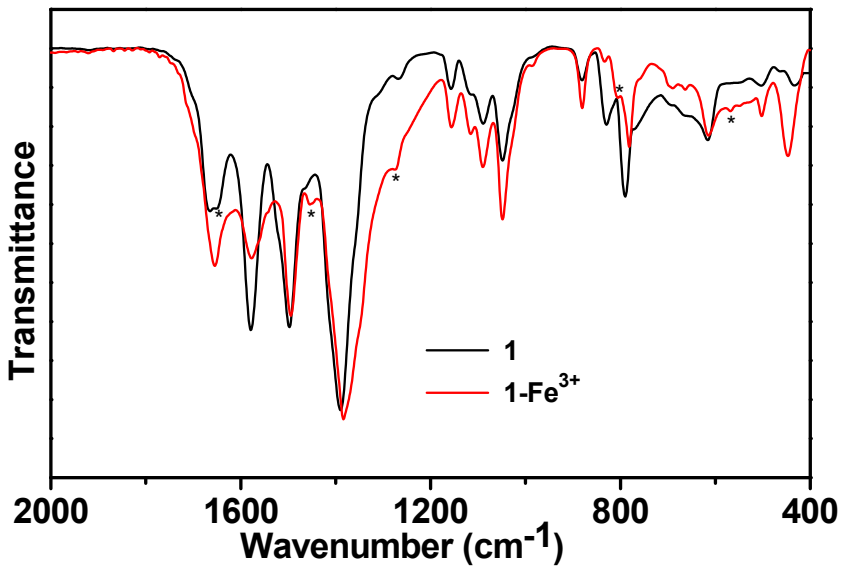

Fig. S21 FT-IR spectra of **1** before and after immersion in $Fe(NO_3)_3$ solutions of DMF(the changes are marked by an asterisk).

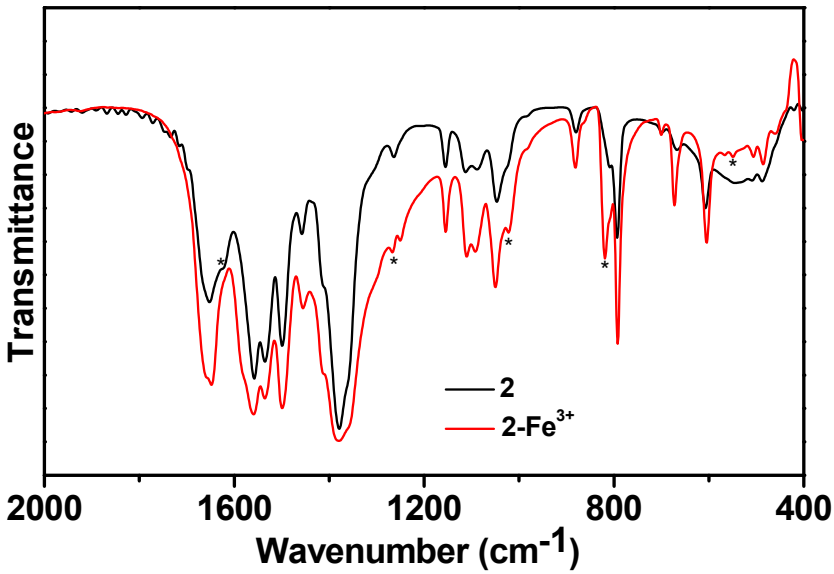

Fig. S22 FT-IR spectra of **2** before and after immersion in $Fe(NO_3)_3$ solutions of DMF(the changes are marked by an asterisk).

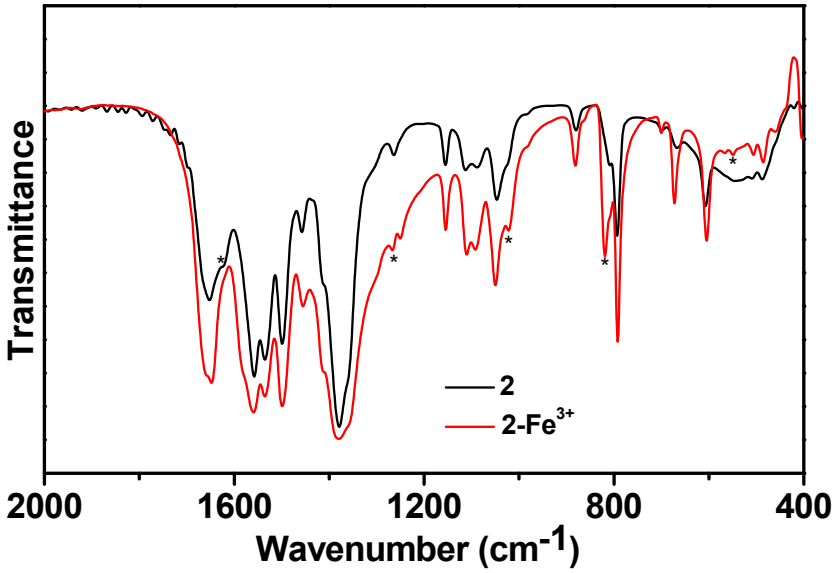

Fig. S23 FT-IR spectra of **3** before and after immersion in $Fe(NO_3)_3$ solutions of DMF(the changes are marked by an asterisk).

Fig. S24 The photographs of **1** and Fe^{3+}-incorporated **1**

Fig. S25 The photographs of **2** and Fe^{3+}-incorporated **2**

Fig. S26 The photographs of **3** and Fe^{3+}-incorporated **3**

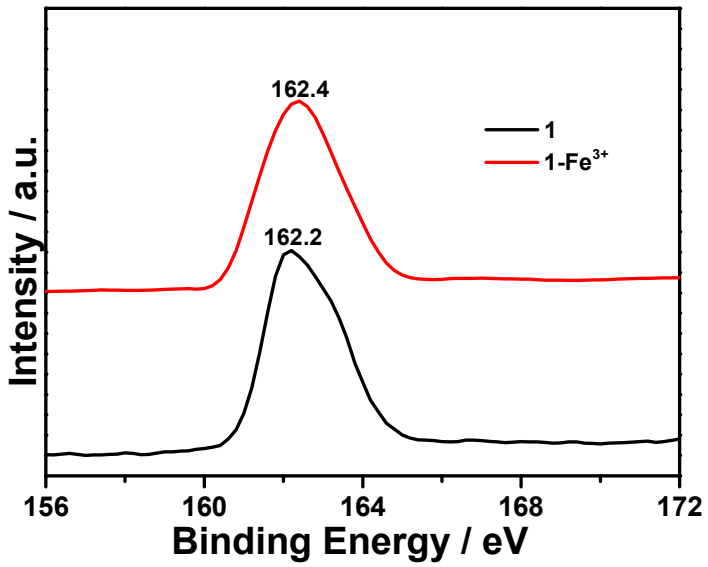

Fig. S27 S2p XPS spectra of **1** before (black) and Fe^{3+}-incorporated **1** (red)

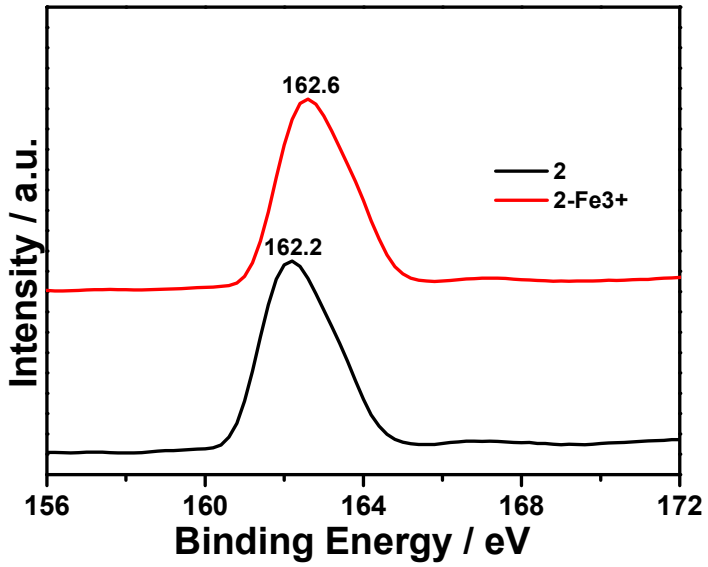

Fig. S28 S2p XPS spectra of **2** before (black) and Fe^{3+}-incorporated **2** (red)

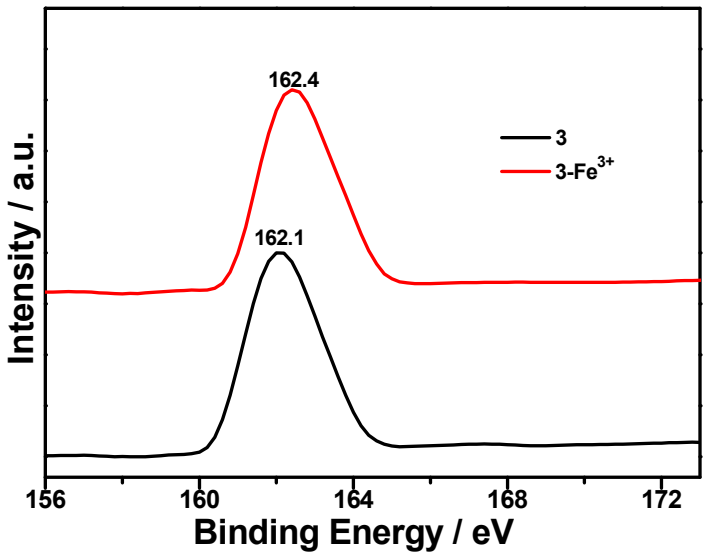

Fig. S29 S2p XPS spectra of **3** before (black) and Fe^{3+}-incorporated **3** (red)

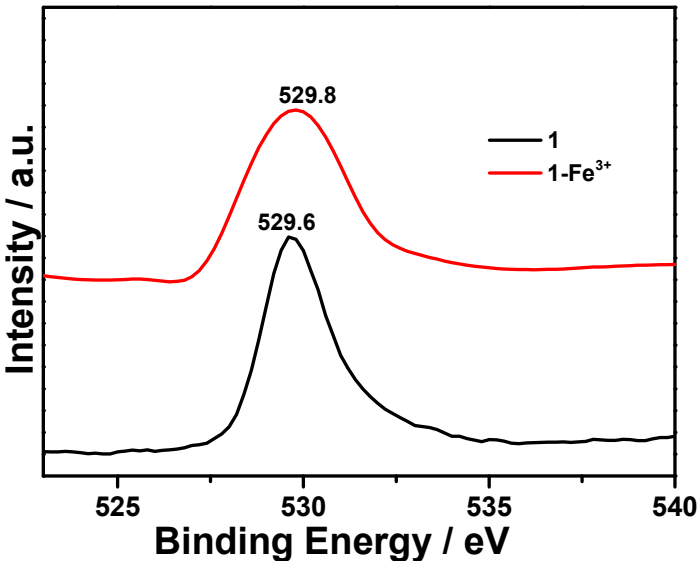

Fig. S30 O1s XPS spectra of **1** before and after immersed in Fe^{3+}

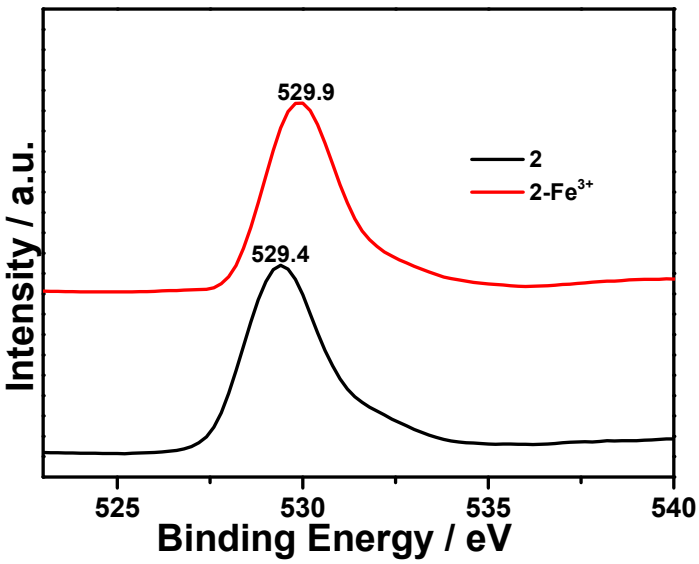

Fig. S31 O1s XPS spectra of **2** before (black) and Fe^{3+}-incorporated **2** (red)

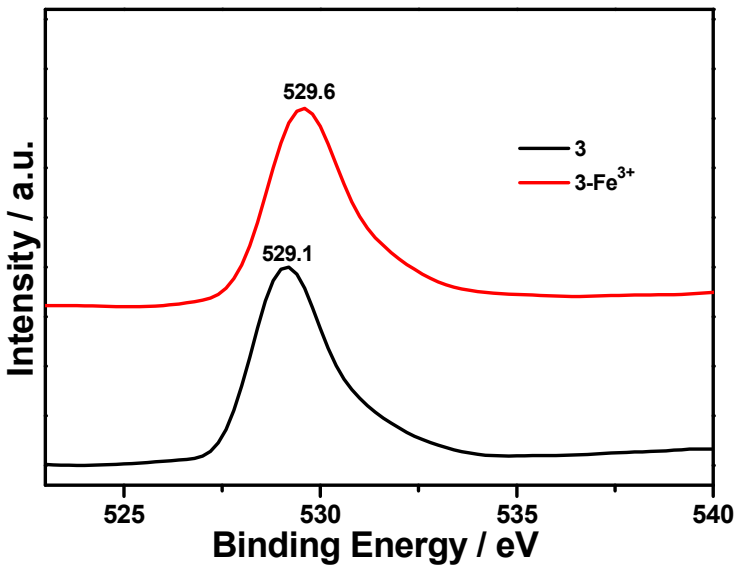

Fig. S32 O1s XPS spectra of **3** before (black) and Fe^{3+}-incorporated **3** (red)

Table S5 The comparison among various fluorescent materials used for detecting Fe^{3+}

Fluorescent materials	**Media (aqueous / organic)**	**Quenching constant *K*sv (M^{-1})**	**Detection limit LOD (M)**	**Ref.**
Mg-CP	H_2O	1.54×10^3	/	2
$[MgZn(1,4\text{-}NDC)_2(DMF)_2$	EtOH	5.0×10^4	/	3
$[Ca_{1.5}(\mu_8\text{-}HL)(DMF)]_n$	H_2O	7.28×10^4	5.91×10^{-6}	4
$\{[M_{g1.5}(\mu_7\text{-}HL)\cdot(H_2O)_2]\cdot 3H_2O\}_n$	H_2O	3.38×10^4	2.20×10^{-5}	4
$[CH_3\text{-}dpb]_2[Mg_3(1,4\text{-}NDC)_4(\mu\text{-}H_2O)_2(CH_3OH)(H_2O)]\cdot 1.5H_2O$	EtOH	1.6×10^4	4.7×10^{-4}	5
$\{[Ca_3L_2(H_2O)_6]\cdot 2H_2O\}_n$	H_2O	3737.8	1.04×10^{-3}	6
$\{[Mg_2(\mu_6\text{-}L)(\mu_2\text{-}OH_2)(H_2O)_4]\cdot DMF\}_n$	H_2O	2.405×10^3	1.68×10^{-3}	7
$[Ca_2(\mu_{10}\text{-}L)(EtOH)]_n$	H_2O	2.342×10^3	1.70×10^{-3}	7
$[Sr(\mu_6\text{-}H_2L)(MeOH)]_n$	H_2O	3.377×10^3	7.47×10^{-4}	7
$\{[Ba_{1.5}(\mu_5\text{-}H_2L)(\mu_4\text{-}H_3L)(H_2O)_3]\cdot 2(H_2O)\}_n$	H_2O	2.643×10^3	1.62×10^{-3}	7
$[Mg_2Zn_2(OH)_2(1,4\text{-}NDC)_3(H_2O)_2]\cdot 6H_2O$	EtOH	1.7×10^4	2.5×10^{-4}	8
$[Mg_2(DMTDC)_2(DMF)_3(H_2O)_2]\cdot 2DMF\cdot 2H_2O$	DMF	8.1×10^4	4.9×10^{-5}	This work
Ca(DMTDC)(DMF)]	DMF	6.9×10^4	2.0×10^{-4}	This work
[Sr(DMTDC)(DMF)]	DMF	2.9×10^4 M	3.7×10^{-4}	This work

Note: Detection limit is obtained from the ratio of 3δ/slope, in which δ is the standard deviation of luminescent intensity of blank solution.

References

1 (a) A. Gilbert and J. Baggott, *Essentials of Molecular Photochemistry*, CRC Press, Boca Raton, FL, 1991; (b) Y. Wang, P. Chen, J. Li, J. Yu, J. Xu, Q. Pan, R. Xu, *Inorg. Chem.*, 2006, **45**, 4764.

2 Y. Liu, J. Xu, X. Y. Tang, Y. S. Ma, R. X. Yuan and R. Matsuda, *Chem. Lett.*, 2019, **48**, 156.

3 Z.-F. Wu and X.-Y. Huang, *ChemistrySelect*, 2018, **3**, 4884.

4 X. S. Lia, J. D. An, H. M. Zhang, J. J. Liu, Y. Li, G. X. Du, X. X. Wu, L. Fei, J. D. Lacoste, Z. Cai, Y. Y. Liu, J. Z. Huo and B. Ding, *Dyes and Pigments*, 2019, **170**, 107631.

5 Z.-F. Wu, L.-K. Gong, and X.-Y. Huang, *Inorg. Chem.*, 2017, **56**, 7397.

6 L.-N. Ma, Y.-K. Lu, W.-J. Shi, L. Hou and Y.-Y Wang, *Inorg. Chem. Comm.*, 2019, **107**, 107490.

7 Y. Liu, L.-N. Ma, W.-J. Shi, Y.-K. Lu, L. Hou and Y.-Y. Wang, *J. Solid State Chem.*, 2019, **277**, 636.

8 Z.-F. Wu and X.-Y. Huang, *Dalton Trans.*, 2017, **46**, 12597.